Phys Chem Minerals (2006) 32: 721–725
DOI 10.1007/s00269-005-0049-7

ORIGINAL PAPER

Shigehiko Tateno · Kei Hirose · Nagayoshi Sata
Yasuo Ohishi

High-pressure behavior of $MnGeO_3$ and $CdGeO_3$ perovskites and the post-perovskite phase transition

Received: 25 July 2005 / Accepted: 24 October 2005 / Published online: 2 December 2005

Abstract The stability and high-pressure behavior of perovskite structure in $MnGeO_3$ and $CdGeO_3$ were examined on the basis of in situ synchrotron X-ray diffraction measurements at high pressure and temperature in a laser-heated diamond-anvil cell. Results demonstrate that the structural distortion of orthorhombic $MnGeO_3$ perovskite is enhanced with increasing pressure and it undergoes phase transition to a $CaIrO_3$-type post-perovskite structure above 60 GPa at 1,800 K. A molar volume of the post-perovskite phase is smaller by 1.6% than that of perovskite at equivalent pressure. In contrast, the structure of $CdGeO_3$ perovskite becomes less distorted from the ideal cubic perovskite structure with increasing pressure, and it is stable even at 110 GPa and 2,000 K. These results suggest that the phase transition to post-perovskite is induced by a large distortion of perovskite structure with increasing pressure.

Keywords Post-perovskite · Perovskite · Phase transition · High-pressure experiment · Diamond-anvil cell

Introduction

Recent experimental and theoretical studies have demonstrated that the orthorhombic $MgSiO_3$ perovskite (space group: *Pbnm*) transforms to a post-perovskite phase (*Cmcm*) above 125 GPa and 2,500 K (e.g., Murakami et al. 2004; Tsuchiya et al. 2004). Similar phase transition was later observed in $MgGeO_3$ and $CaIrO_3$ at ~63 and ~1 GPa, respectively (Hirose et al. 2005a; Hirose and Fujita 2005). The chemical variations that adopt post-perovskite structure are little known yet. Here, we examined the stability and compression behavior of perovskite in both $MnGeO_3$ and $CdGeO_3$ at high pressure and temperature by a combination of laser-heated diamond-anvil cell (LHDAC) techniques and synchrotron X-ray diffraction measurements.

$MnGeO_3$ crystallizes with an orthopyroxene structure at ambient condition. It transforms to clinopyroxene and then to ilmenite structure at 3.0 GPa and 973 K (Ringwood and Seabrook 1963; Ross and Reynard 1991). The $MnGeO_3$ ilmenite further transforms to orthorhombic perovskite structure at about 25 GPa (Liu 1976; Ito and Matsui 1979). The high-pressure polymorphs of $CdGeO_3$ have been also well studied (e.g., Ringwood and Major 1967; Prewitt and Sleight 1969; Susaki et al. 1985). Akaogi and Navrotsky (1987) reported that $CdGeO_3$ garnet, ilmenite, and perovskite are formed at 4.0, 7.5, and 13.5 GPa, respectively. These high-pressure phase transition sequences of $MnGeO_3$ and $CdGeO_3$ are similar to those of $MgSiO_3$ and $MgGeO_3$.

Experimental techniques

Starting materials of $MnGeO_3$ and $CdGeO_3$ were synthesized by using Boyd-England-type piston cylinder apparatus. For $MnGeO_3$, a mixture of MnO and GeO_2 powder was loaded into a graphite capsule and held at 2.0 GPa and 1,323 K for 20 h. This P–T condition is within a stability of $MnGeO_3$ clinopyroxene (Ringwood and Seabrook 1963). The excess of GeO_2 in the run product was confirmed by X-ray diffraction measurement. For $CdGeO_3$, the garnet form was synthesized at

S. Tateno (✉) · K. Hirose
Department of Earth and Planetary Sciences, Tokyo Institute of Technology, 2-12-1 Ookayama, 152-8551 Meguro, Tokyo, Japan
E-mail: stateno@geo.titech.ac.jp
Tel.: +81-3-57342618
Fax: +81-3-57343538

N. Sata · K. Hirose
Institute for Research on Earth Evolution, Japan Agency for Marine-Earth Science and Technology, Yokosuka, Kanagawa, Japan

Y. Ohishi
Japan Synchrotron Radiation Research Institute, Mikazuki-cho, Sayo-gun, Hyogo, Japan

2.0 GPa and 1,323 K in 93 h from an equimolar mixture of CdO and GeO_2 powder.

These starting materials were well ground to fine powder and were mixed with platinum black that served both as an internal pressure standard and a laser absorber. The sample mixture was loaded into a 100-μm hole drilled in a Re-gasket together with insulation layers. We used NaCl and pure $CdGeO_3$ as insulation layers in the $MnGeO_3$ and $CdGeO_3$ experiments, respectively. They were compressed with 300-μm culet diamond anvils. Heating was made by a focussed multimode continuous wave Nd:YAG laser using the double-side heating technique. Temperature was measured from one side by the spectroradiometric method (Watanuki et al. 2001).

Angle dispersive X-ray diffraction spectra were collected on an imaging plate at BL10XU of SPring-8. Exposure time was 2–5 min. An incident X-ray beam was monochromatized to a wavelength of 0.4136–0.4138 Å. The X-ray beam was collimated to 20 μm in diameter. Two-dimensional X-ray diffraction image was integrated as a function of two-theta in order to give a conventional one-dimensional diffraction profile using the fit-2D program (Hammersley 1996).

The uncertainty in temperature within the 20 μm area from which X-ray diffraction was collected was about ±10% (e.g., Kurashina et al. 2004). Pressure was determined using the equation of state of platinum proposed by Holmes et al. (1989) using both (111) and (200) lines. The uncertainty in pressure was less than ±0.2 GPa at room temperature and ±1.1 to 1.4 GPa at 1,520–2,150 K. The larger error at high temperature was derived mainly from large uncertainty in temperature in the application of *P–V–T* equation of state. The diffraction patterns of the sample were repeatedly collected at high temperatures and at room temperature before and after heating.

Results

$MnGeO_3$

We conducted two separate sets of experiments at pressures between 46 and 77 GPa and temperatures between 1,520 and 2,150 K. In the first run, the sample was compressed at room temperature to 32 GPa and was subsequently heated for 7 min at 46–48 GPa and 1,520–1,830 K. The diffraction peaks of orthorhombic perovskite (space group: *Pbnm*) immediately appeared within 2 min and did not change with further heating. The XRD pattern also included peaks from platinum, NaCl, and $CaCl_2$-type GeO_2 phase (Ono et al. 2003) (Fig. 1a).

We compressed this sample further to 61 GPa at room temperature. The diffraction peaks of perovskite still remained. In the subsequent heating to 1,680–1,960 K at 73–77 GPa, 22 new peaks appeared within 2 min. The XRD pattern obtained after heating intermittently for a total of 74 min is shown in Fig. 1b. The Rietveld analysis shows that these new peaks are assigned to $CaIrO_3$-type post-perovskite (*Cmcm*) and α-PbO_2-type GeO_2 phases (Izumi and Ikeda 2000). The unit-cell volume of post-perovskite phase is smaller by 1.6% than that of coexisting perovskite at 72 GPa and 1,720 K. This is consistent with the previous observations in $MgSiO_3$ and $MgGeO_3$ (Murakami et al. 2004; Hirose et al. 2005a). Upon decompression to ambient condition, the peaks of post-perovskite disappeared. The $MnGeO_3$ post-perovskite phase is pressure-unquenchable similar to $MgGeO_3$ (Hirose et al. 2005a).

In the second set of experiments, the sample was compressed to 45 GPa at room temperature. We then heated the sample to 1,620–2,150 K at 58–59 GPa for 20 min. The peaks both of perovskite and post-perovskite appeared within 5 min. However, the perovskite peaks grew with time, while those of post-perovskite became weak. These observations suggest that this *P–T* condition is within stability of perovskite but is very close to the phase transition boundary. The stabilities of perovskite and post-perovskite phases are summarized in Fig. 2. Phase boundary should be located around 60 GPa at 1,800 K, which is much lower than the 125 GPa at 2,500 K in $MgSiO_3$. This is close to the post-perovskite phase transition boundary in $MgGeO_3$ (~63 GPa at 1,800 K) (Hirose et al. 2005a).

$CdGeO_3$

In the first set of experiments on $CdGeO_3$, the sample was initially compressed to 23 GPa at room temperature. The diffraction peaks from the starting material of tetragonal garnet remained before heating. After heating at ~1,500 K for 10 min, orthorhombic perovskite was formed, although the garnet phase still remained in the diffraction pattern. The pressure decreased to 8.9 GPa after quenching to room temperature, due to a stress relaxation in the sample chamber. We again compressed this sample to 22 GPa at room temperature and reheated to ~1,700 K for 17 min at 23 GPa. The peaks from garnet became weak relative to those of perovskite during heating. This sample was further compressed to 67 GPa at room temperature. The diffraction peaks of garnet disappeared, and the XRD pattern included peaks only from perovskite and platinum before heating. The pattern did not change by heating to 2,000 K at 62 GPa.

In the second run, the sample was directly compressed to 100 GPa at room temperature. The perovskite phase was obtained after heating to 2,000 K at 110 GPa for 25 min. The perovskite peaks were relatively broad at this pressure range.

Distortion of perovskite structure and the phase transition

The changes in unit-cell parameters ($a_c = a/\sqrt{2}$, $b_c = b/\sqrt{2}$, and $c_c = c/2$) of orthorhombic perovskites ($MgGeO_3$,

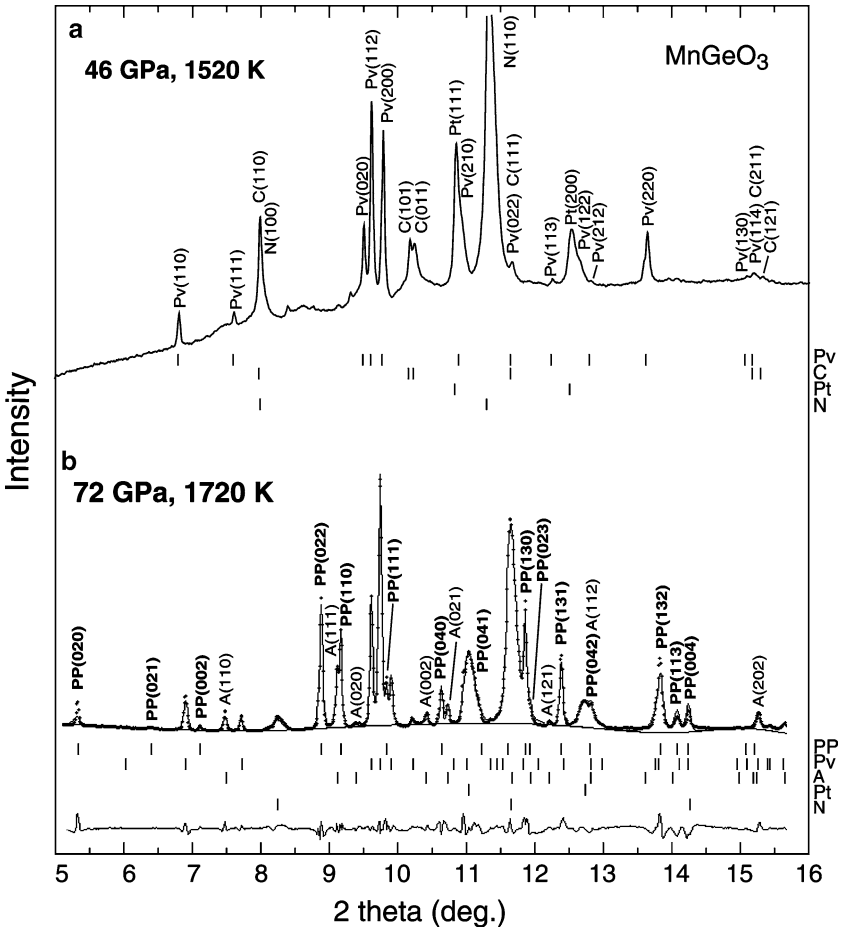

Fig. 1 **a** X-ray diffraction pattern of $MnGeO_3$ at 46 GPa and 1,520 K. **b** Observed (pluses) and calculated pattern at 72 GPa and 1,720 K. *Small ticks* show the peak positions of each phase. *Pv* perovskite, *PP* post-perovskite, *Pt* platinum, *N* B2-type sodium chloride, *C* $CaCl_2$-type GeO_2, *A* α-PbO_2-type GeO_2. Unit-cell parameters are: **a** $a = 4.848(3)$ Å, $b = 4.995(3)$ Å, and $c = 7.001(4)$ Å for Pv, and **b** $a = 2.703(1)$ Å, $b = 8.921(3)$ Å, and $c = 6.668(1)$ Å for PP and $a = 4.792(3)$ Å, $b = 4.933(2)$ Å, and $c = 6.915(6)$ Å for Pv

$MnGeO_3$, and $CdGeO_3$) are shown in Fig. 3 as a function of pressure at 300 K. The data of $MgGeO_3$ perovskite are from Hirose et al. (2005a). Both in $MgGeO_3$ and $MnGeO_3$ perovskites, the values of a_c, b_c, and c_c diverge more with increasing pressure, indicating that the structural distortion from the ideal cubic perovskite structure is enhanced with pressure. This is also suggested from the change in the axial ratios (b_c/a_c and c_c/a_c), which increases with pressure in both $MgGeO_3$ and $MnGeO_3$ perovskites (Fig. 4). The b_c/a_c and c_c/a_c ratios reach 1.060 and 1.036 in $MgGeO_3$ perovskite when it transforms to post-perovskite at 63 GPa. Similarly, in $MnGeO_3$ perovskite, the b_c/a_c and c_c/a_c ratios are 1.034 and 1.021 at 61 GPa near the post-perovskite phase transition boundary.

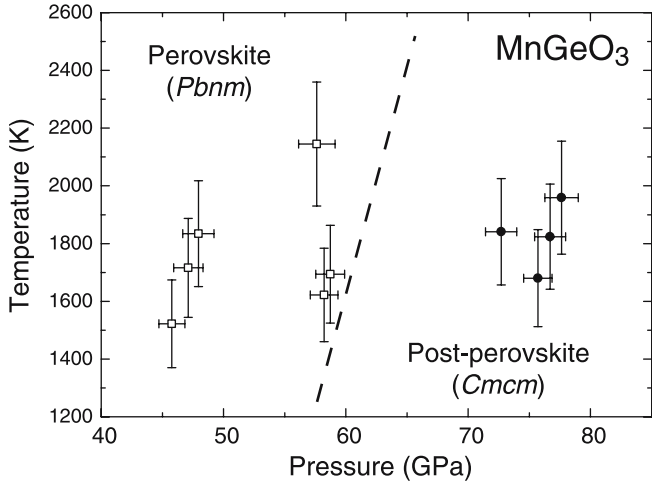

Fig. 2 Phase diagram of $MnGeO_3$. *Open squares* perovskite; *closed circles* post-perovskite. Phase boundary is tentatively drawn with a Clapeyron slope of +7.5 MPa/K as predicted by Tsuchiya et al. (2004) for $MgSiO_3$

In contrast, for $CdGeO_3$ perovskite, the lattice parameters tend to converge with increasing pressure (Figs. 3, 4), suggesting that the perovskite structure becomes less distorted at higher pressures. The b_c/a_c and c_c/a_c ratios are close to unity at 55 GPa, and the post-perovskite phase transition does not occur even at 110 GPa and 2,000 K. These observations strongly suggest that post-perovskite phase transition is induced by a large distortion of perovskite structure with increasing pressure. The post-perovskite phase transition is most unlikely to occur in $CdGeO_3$.

The distortion in $MgGeO_3$ and $MnGeO_3$ perovskites is possibly caused by the small sized Mg^{2+} and Mn^{2+} relative to Cd^{2+}. Because their sites in post-perovskite are smaller than those in perovskite (Iitaka et al. 2004; Tsuchiya et al. 2004), they fit in post-perovskite better than in perovskite.

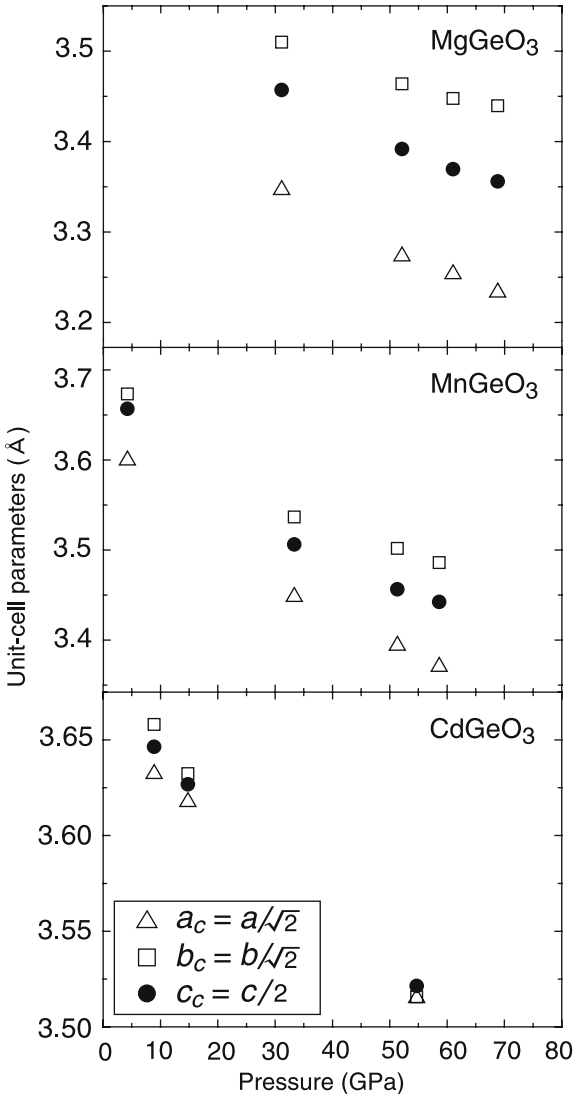

Fig. 3 Changes in the unit-cell parameters at 300 K as a function of pressure for $MgGeO_3$, $MnGeO_3$, and $CdGeO_3$ perovskites. Errors are smaller than the symbol size

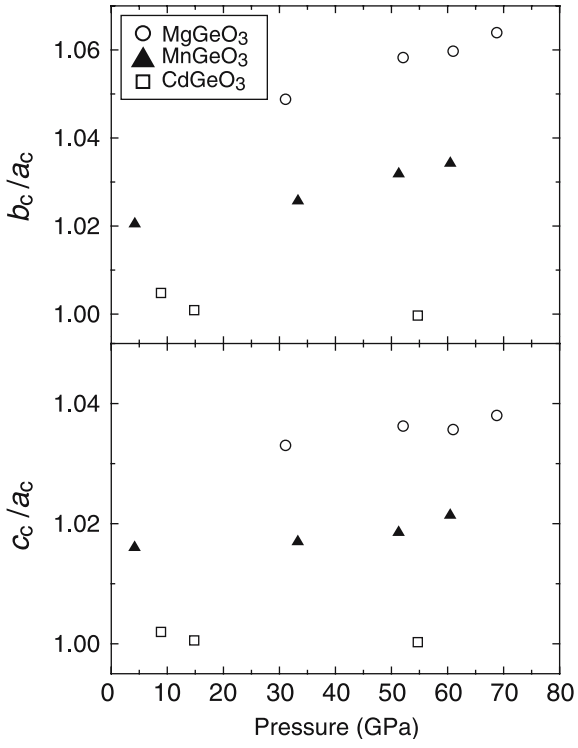

Fig. 4 Changes in the axial ratios of b_c/a_c and c_c/a_c at 300 K as a function of pressure for $MgGeO_3$, $MnGeO_3$, and $CdGeO_3$ perovskites

ABO_3 compounds with post-perovskite structure

It is well known that a number of $A^{2+}B^{4+}O_3$ compounds adopt perovskite structure. In contrast, only $MgSiO_3$, $MgGeO_3$, $MnGeO_3$, and $CaIrO_3$ perovskites are so far reported to transform to the post-perovskite structure. These compounds are illustrated in Fig. 5 as functions of ionic radii of sixfold-coordinated "A" and "B" cations (Shannon and Prewitt 1969). The tolerance factors $t = (r_A + r_O)/\sqrt{2}(r_B + r_O)$ are also shown on this diagram, where r_A and r_B are the ionic radii of eightfold-coordinated "A" cation and sixfold-coordinated "B" cation respectively and r_O is the ionic radius of oxygen anion.

Previous experimental studies by Andraut and Poirier (1991) and Ross and Angel (1999) demonstrated that the distortion of orthorhombic $CaGeO_3$ perovskite from ideal cubic symmetry decreases with increasing pressure up to 10 GPa. Therefore, the post-perovskite phase transition is not likely to occur in $CaGeO_3$ with increasing pressure, similarly to $CdGeO_3$. The cubic

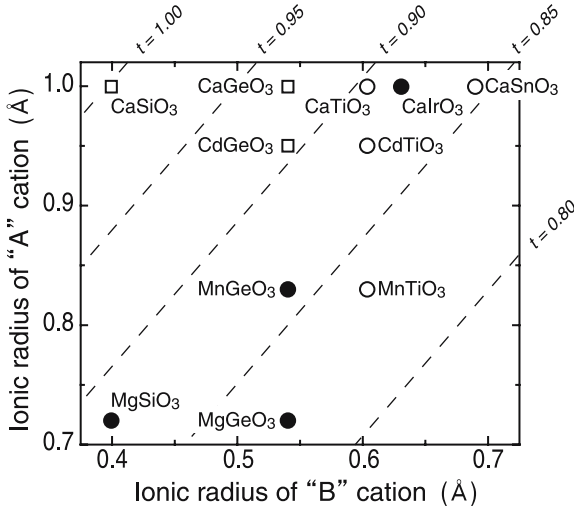

Fig. 5 Goldshmidt diagram showing the ABO_3 compounds with post-perovskite structure. The ionic radii are from Shannon and Prewitt (1969). *Broken lines* indicate contours of the tolerance factors, *t*; *closed circles*, compounds in which perovskite phase transforms to post-perovskite with increasing pressure; *open circles*, compounds in which perovskite becomes unstable above 30–70 GPa but transforms to the structure other than post-perovskite; *open squares*, compounds whose structure becomes less distorted with increasing pressure and is unlikely to transform to post-perovskite or compound that is stable at least to 134 GPa ($CaSiO_3$)

$CaSiO_3$ perovskite is stable, at least to 134 GPa and 2,300 K in a natural basalt composition (Hirose et al. 2005b).

In addition, we examined the phase transition of $CaTiO_3$, $CdTiO_3$, $MnTiO_3$, and $CaSnO_3$ perovskites at high pressures (Fig. 5), on the basis of in situ X-ray diffraction measurements which were same as that in this study. Preliminary results indicate that all of these perovskites do not transform into the post-perovskite structure at least to ~70 GPa (Tateno et al. 2004). In both perovskite and post-perovskite structures, the coordination numbers are eight for A^{2+} and six for B^{4+} ions. The coordination numbers of Ti^{4+} and Sn^{4+} increase from six to seven or eight at relatively low pressures (Haines and Léger 1993; Haines et al. 1996). The change in cation coordination number may lead to the phase transition of titanate and stannate perovskites into different structures other than post-perovskite.

These are summarized in Fig. 5. The chemical variation in $A^{2+}B^{4+}O_3$ compounds that adopt post-perovskite structure cannot be simply explained by the cation ionic radii. The structural change between perovskite and post-perovskite with chemical composition is not clear even at ambient condition; both $CaTiO_3$ and $CaSnO_3$ have perovskite structure, whereas $CaIrO_3$ exhibits post-perovskite structure. Further studies are necessary to clarify this issue.

Acknowledgements The in situ X-ray experiments were carried out at SPring-8 (proposal no. 2004A3013-LD2-np and 2004B4013-LD2-np). We thank Y. Kuwayama for his assistance in the Rietveld analysis. We are grateful to K. Kawamura for his constructive comments throughout this study. We also thank E. Takahashi for the use of the piston cylinder apparatus in his laboratory. The constructive reviews by R. Boehler and an anonymous referee were helpful in improving the manuscript. S.T. was supported by the 21st century COE program of the Japan Society for the Promotion of Science.

References

Akaogi M, Navrotsky A (1987) Calorimetric study of high-pressure phase transitions among the $CdGeO_3$ polymorphs (pyroxenoid, garnet, ilmenite, and perovskite structures). Phys Chem Miner 14:435–440

Andraut D, Poirier JP (1991) Evolution of the distortion of perovskites under pressure: an EXAFS study of $BaZrO_3$, $SrZrO_3$, and $CaGeO_3$. Phys Chem Miner 18:91–105

Haines J, Léger JM (1993) X-ray diffraction study of TiO_2 up to 49 GPa. Physica B 192:233–237

Haines J, Léger JM, Schulte O (1996) $Pa\bar{3}$ modified fluorite-type structures in metal dioxides at high pressure. Science 271:629–631

Hammersley J (1996) Publication No.F98HA01T, ESRF, Grenoble, France

Hirose K, Fujita Y (2005) Clapeyron slope of the post-perovskite phase transition in CaIrO3. Geophys Res Lett 32:L13313. DOI 10.1029/2005GL023219

Hirose K, Kawamura K, Ohishi Y, Tateno S, Sata N (2005a) Stability and equation of state of $MgGeO_3$ post-perovskite phase. Am Mineral 90:262–265

Hirose K, Takafuji N, Sata N, Ohishi Y (2005b) Phase transition and density of subducted MORB crust in the lower mantle. Earth Planet Sci Lett 237:239–251

Holmes NC, Moriarty JA, Gathers GR, Nellis WJ (1989) The equation of state of platinum to 660 GPa (6.6 Mbar). J Appl Phys 66:2962–2967

Iitaka T, Hirose K, Kawamura K, Sata N, Ohishi Y (2004) The elasticity of the $MgSiO_3$ post-perovskite phase in the Earth's lower mantle. Nature 430:442–444

Ito E, Matsui Y (1979) High-pressure transformations in silicates, germanates, and titanates with ABO_3 stoichiometry. Phys Chem Mineral 4:265–273

Izumi F, Ikeda T (2000) A Rietveld-analysis program RIETAN-98 and its applications to zeolites. Mater Sci Forum 321–324:198–203

Kurashina T, Hirose K, Ono S, Sata N, Ohishi Y (2004) Phase transition in Al-bearing $CaSiO_3$ perovskite: implications for seismic discontinuities in the lower mantle. Phys Earth Phys Inter 145:67–74

Liu LG (1976) High-pressure phase of Co_2GeO_4, Ni_2GeO_4, Mn_2GeO_4 and $MnGeO_3$: implications for the germinate-silicate modeling scheme and the earth's mantle. Earth Planet Sci Lett 31:393–396

Murakami M, Hirose K, Kawamura K, Sata N, Ohishi Y (2004) Post-perovskite phase transition in $MgSiO_3$. Science 304:855–858

Ono S, Tsuchiya T, Hirose K, Ohishi Y (2003) Phase transition between the $CaCl_2$-type and α-PbO_2-type structures of germanium dioxide. Phys Rev B 68:134108

Prewitt CT, Sleight AW (1969) Garnet-like structures of high-pressure cadmium germanate and calcium germanate. Science 163:386–387

Ringwood AE, Major A (1967) Some high-pressure transformations of geophysical significance. Earth Planet Sci Lett 2:106–110

Ringwood AE, Seabrook M (1963) High-pressure phase transformations in germanate pyroxenes and related compounds. J Geophys Res 68:4601–4608

Ross NL, Angel RJ (1999) Compression of $CaTiO_3$ and $CaGeO_3$ perovskites. Am Mineral 84:277–281

Ross NL, Reynard B (1991) Structure of high-pressure $MnGeO_3$ ilmenite. Acta Crystallogr C47:1794–1796

Shannon RD, Prewitt CT (1969) Effective ionic radii in oxide and fluorides. Acta Crystallogr B25:925–946

Susaki J, Konno M, Akimoto S (1985) High-pressure synthesis and structural refinement of $CdGeO_3$ ilmenite. Z Kristallogr 171:243–252

Tateno S, Hirose K, Sata N, Ohishi Y (2004) Stability of post-perovskite phase in analogue materials to MgSiO3. Eos Trans AGU 85(47) Fall meeting Suppl Abstract MR23A-0183

Tsuchiya T, Tsuchiya J, Umemoto K, Wentzcovitch RM (2004) Phase transition in $MgSiO_3$ perovskite in the earth's lower mantle. Earth Planet Sci Lett 224:241–248

Watanuki T, Shimomura O, Kondo T, Isshiki M (2001) Construction of laser-heated diamond anvil cell system for in situ X-ray diffraction study at SPring-8. Rev Sci Instrum 72:1289–1292